university of groningen

University Medical Center Groningen

University of Groningen

Experimental determination of the JPI components of the spin-dipole resonance in 12B

de Huu, Marc Alexander

IMPORTANT NOTE: You are advised to consult the publisher's version (publisher's PDF) if you wish to cite from it. Please check the document version below.

Document Version
Publisher's PDF, also known as Version of record

Publication date:
2004

Link to publication in University of Groningen/UMCG research database

Citation for published version (APA):
de Huu, M. A. (2004). *Experimental determination of the JPI components of the spin-dipole resonance in 12B*. s.n.

Copyright
Other than for strictly personal use, it is not permitted to download or to forward/distribute the text or part of it without the consent of the author(s) and/or copyright holder(s), unless the work is under an open content license (like Creative Commons).

The publication may also be distributed here under the terms of Article 25fa of the Dutch Copyright Act, indicated by the "Taverne" license. More information can be found on the University of Groningen website: https://www.rug.nl/library/open-access/self-archiving-pure/taverne-amendment.

Take-down policy
If you believe that this document breaches copyright please contact us providing details, and we will remove access to the work immediately and investigate your claim.

Downloaded from the University of Groningen/UMCG research database (Pure): http://www.rug.nl/research/portal. For technical reasons the number of authors shown on this cover page is limited to 10 maximum.

Download date: 29-10-2022

3. Theory

This chapter introduces some of the theoretical tools used in the description of the present experiment. First an overview of the effective interaction and how it leads to spin-isospin excitations is given. I will then dwell on one of them: the spin-dipole resonance (SDR). A description of the tools used to study spin-isospin excitations and some related observables will be derived. A thorough review of nuclear spin-isospin excitations can be found in the review article of Osterfeld [21], on which the first part of this chapter is based.

3.1 The effective nucleon interaction

To interpret scattering data, knowledge of the interaction between the probe (projectile) and the nucleus is essential. In the case of nucleon-induced reactions, the interaction stems mainly from the strong force, which allows one to investigate many different types of excitations due to the spin and isospin structure of the nucleon-nucleon (NN) interaction.

Because of the short range of the strong force, and at a sufficiently high incident energy ($\approx$ 100 MeV/u), the projectile-target interaction can be approximated by an effective interaction $V_{pt} = \sum_{j=1}^{A} V_{pj}$ between the projectile nucleon p and the nucleons j in the target, where V_{pj} represents the bare NN interaction. This approximation is known as the *impulse approximation* (IA) and relies on the fact that the projectile interacts with one nucleon in the target nucleus, without any influence of the surrounding nucleons. For energies below 100 MeV/u, nuclear medium effects, like multiple scattering and Pauli blocking, start playing a role and the effective interaction so constructed is known as *Brueckner's scattering G matrix* [22].

In the IA, the effective interaction between the incident nucleon and each of the target nucleons is taken to be the kinematically corrected free NN t_F matrix [2, 23]. A parametrisation of the NN t_F matrix between bombarding energies of 50 and 1000 MeV/u for use in actual calculations has been determined by Franey and Love [2, 23]. They write the effective interaction as a sum of central (C), spin-orbit (LS) and tensor (T) terms in

the following spin-isospin decomposition

$$\begin{aligned} V_{pj}(\boldsymbol{r}) &= V_0^C(r) + V_\sigma^C(r)\ \boldsymbol{\sigma}_p \cdot \boldsymbol{\sigma}_j + V_\tau^C(r)\ \boldsymbol{\tau}_p \cdot \boldsymbol{\tau}_j \\ &+ V_{\sigma\tau}^C(r)\ \boldsymbol{\sigma}_p \cdot \boldsymbol{\sigma}_j\ \boldsymbol{\tau}_p \cdot \boldsymbol{\tau}_j \\ &+ [V^{LS}(r) + V_\tau^{LS}(r)\ \boldsymbol{\tau}_p \cdot \boldsymbol{\tau}_j]\ \boldsymbol{L}_{pj} \cdot \boldsymbol{S} \\ &+ [V^T(r) + V_\tau^T(r)\ \boldsymbol{\tau}_p \cdot \boldsymbol{\tau}_j]\ \boldsymbol{S}_{pj}(\hat{\boldsymbol{r}})\ , \end{aligned} \tag{3.1}$$

where $\boldsymbol{r} = \boldsymbol{r}_p - \boldsymbol{r}_j$ is the relative coordinate of the two interacting nucleons, $\boldsymbol{L}_{pj} = (\boldsymbol{r}_p - \boldsymbol{r}_j) \times (\boldsymbol{k}_p - \boldsymbol{k}_j)/2$ is the relative angular momentum operator between the projectile p and target nucleon j, $\boldsymbol{S} = \boldsymbol{s}_p + \boldsymbol{s}_j$ is the total two-nucleon spin and $\boldsymbol{S}_{pj}(\hat{\boldsymbol{r}}) = 3\boldsymbol{\sigma}_p \cdot \hat{\boldsymbol{r}} \boldsymbol{\sigma}_j \cdot \hat{\boldsymbol{r}} - \boldsymbol{\sigma}_p \cdot \boldsymbol{\sigma}_j$ is the tensor operator. The complex amplitudes V of the central and spin-orbit components are taken to be sums of Yukawa forms

$$V_{pj}(r) = \sum_{i=1}^{N} V_i \frac{\exp(-r/R_i)}{r/R_i}\ . \tag{3.2}$$

The radial shape of the tensor term is taken to be r^2 times a sum of Yukawa terms. The force ranges R_i and strengths V_i are free parameters and are determined from a best fit to the t_F matrix of eq. 3.1, or more specifically, until

$$t_F(E_{CM}, \boldsymbol{q}) = \int d\boldsymbol{r} \exp(-i\boldsymbol{k'} \cdot \boldsymbol{r})\ V_{pj}(\boldsymbol{r})[1 + (-1)^l P^x] \exp(i\boldsymbol{k} \cdot \boldsymbol{r})\ , \tag{3.3}$$

is within satisfactory limits, where E_{CM} is the energy in the two-nucleon centre-of-mass frame and $\boldsymbol{q} = \boldsymbol{k} - \boldsymbol{k'}$. The space-exchange operator, P^x, and $(-1)^l$ (l is the relative angular momentum in the N-N system) ensure antisymmetrisation. The energy dependence of the central part of the effective interaction at zero-momentum transfer ($q = 0$) is shown in figure 3.1. One sees that the best incoming beam energy region to study isovector spin-flip excitations at vanishing momentum transfer lies between 150 and 400 MeV/u, since at these energies, the isoscalar central part of the effective interaction goes through a minimum and the isovector spin-flip part is the second-dominant one.

The spin-isospin dependence of the effective interaction is explicit in eq. 3.1 and can be used for the description of inelastic-scattering processes. All terms that involve the spin operators $\boldsymbol{\sigma}_p \cdot \boldsymbol{\sigma}_j$, $\boldsymbol{S}$ or $\boldsymbol{S}_{pj}$ produce spin-flip transitions in the projectile and in the target, and all terms that involve the isospin operator $\boldsymbol{\tau}_p \cdot \boldsymbol{\tau}_j$ induce isospin transitions. For charge-exchange reactions, isospin excitations of the target are mediated by the operators $\boldsymbol{\tau}_\pm$.

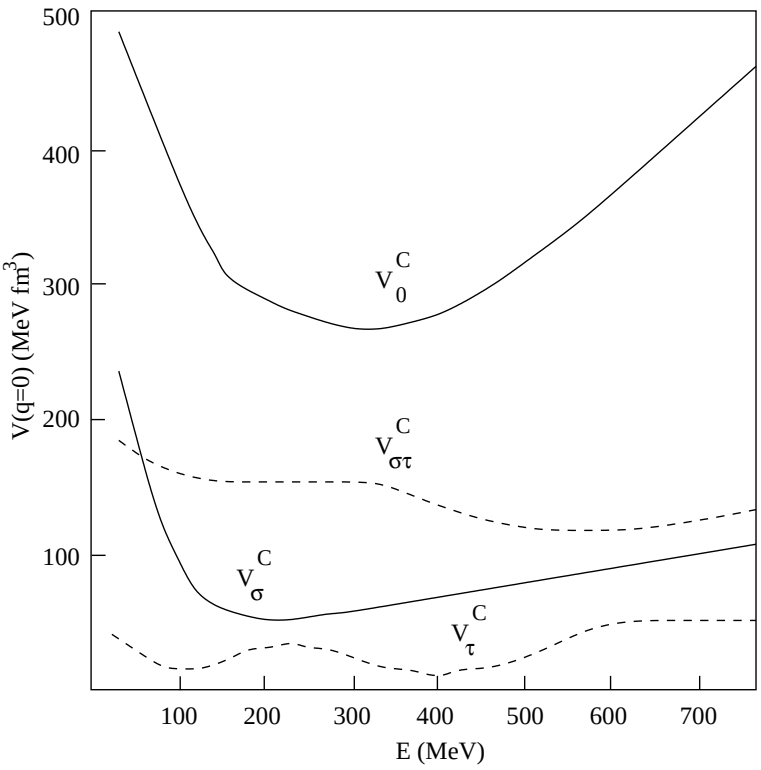

Figure 3.1: Energy dependence of the central components of the effective t_F matrix at zero-momentum transfer, taken from ref. [24].

3.2 Spin-isospin excitations

The presence of spin-isospin dependent terms in the effective interaction of eq. 3.1 gives rise to spin-isospin excitations. If one expands the isovector part of V_{pj} in terms of its Fourier components, one gets [21] (I have added the spin-orbit term)

$$\begin{aligned} V_{pj}^{\tau}(\boldsymbol{r}_p, \boldsymbol{r}_j) &= \frac{1}{(2\pi)^3} \int d\boldsymbol{q}\ \exp(-i\boldsymbol{q}\cdot\boldsymbol{r}_p) \\ &\quad [V_\tau^C(q) + V_{\sigma\tau}^C(q)\boldsymbol{\sigma}_p\cdot\boldsymbol{\sigma}_j - iV_\tau^{LS}(q)\boldsymbol{S}\cdot\hat{\boldsymbol{n}} - V_\tau^T(q)\boldsymbol{S}_{pj}(\hat{\boldsymbol{q}})] \\ &\quad \exp(i\boldsymbol{q}\cdot\boldsymbol{r}_j)\ \boldsymbol{\tau}_p\cdot\boldsymbol{\tau}_j\ , \end{aligned} \tag{3.4}$$

where the tensor operator $\boldsymbol{S}_{pj}$ is defined by $\boldsymbol{S}_{pj} = 3\boldsymbol{\sigma}_p\cdot\hat{\boldsymbol{q}}\boldsymbol{\sigma}_j\cdot\hat{\boldsymbol{q}} - \boldsymbol{\sigma}_p\cdot\boldsymbol{\sigma}_j$. The coordinate system used is the one in which the unit vectors $[\hat{\boldsymbol{Q}}, \hat{\boldsymbol{q}}, \hat{\boldsymbol{n}}]$ form a

right-handed coordinate system with $\boldsymbol{Q} = \boldsymbol{k'} + \boldsymbol{k}$, $\boldsymbol{q} = \boldsymbol{k} - \boldsymbol{k'}$ and $\hat{\boldsymbol{n}} = \hat{\boldsymbol{q}} \times \hat{\boldsymbol{Q}}$. In the remaining part of this section, we will confine our attention to the central and tensor parts of the interaction, since they are generally more important than the spin-orbit interaction in producing isovector excitations [2].

Another convenient way of writing the spin-dependent interaction terms of eq. 3.4 (without the spin-orbit part) is in the longitudinal and transverse representation

$$V_{pj}^{\tau}(\boldsymbol{q}) = \Big[V_{\tau}^{C}(q) + V_{\tau}^{l}(q)\ \boldsymbol{\sigma}_p \cdot \hat{\boldsymbol{q}}\ \boldsymbol{\sigma}_j \cdot \hat{\boldsymbol{q}} + V_{\tau}^{t}(q)\ (\boldsymbol{\sigma}_p \times \hat{\boldsymbol{q}}) \cdot (\boldsymbol{\sigma}_j \times \hat{\boldsymbol{q}}) \Big] \boldsymbol{\tau}_p \cdot \boldsymbol{\tau}_j\ , \quad (3.5)$$

where V_{τ}^{l} and V_{τ}^{t} are the spin-longitudinal (l) and spin-transverse (t) isovector components of the interaction given by

$$V_{\tau}^{l} = V_{\sigma\tau}^{C}(q) - 2V_{\tau}^{T}(q)\ , \quad (3.6)$$

$$V_{\tau}^{t} = V_{\sigma\tau}^{C}(q) + V_{\tau}^{T}(q)\ . \quad (3.7)$$

It should be noted that the electromagnetic interaction measures only the transverse spin response of nuclei ($\boldsymbol{\sigma} \times \boldsymbol{q}$) and is therefore (in first order) blind to spin-longitudinal excitations because of the transverse character of the one-photon exchange [21]. Moreover, excitation of spin-longitudinal transitions is forbidden by particles with zero spin such as pions and alpha particles.

A further specification of the states that can be excited is obtained by performing a multipole expansion of eq. 3.4. Expanding the plane waves in eq. 3.4 into partial waves and coupling the orbital (L) and spin (S) angular momenta to a total angular momentum J leads to an expansion of V_{pj} in terms of the tensor operators

$$M_{LSJ,\mu}(q\boldsymbol{r}, O_S) = j_L(qr)\ [i^L\ Y_L(\hat{\boldsymbol{r}}) \otimes O_S]^J\ \boldsymbol{\tau}_{\mu}\ , \quad (3.8)$$

where $O_{S=0} = 1$, $O_{S=1} = \boldsymbol{\sigma}$,

$$\boldsymbol{\tau}_{\mu} = \begin{cases} \mp\frac{1}{\sqrt{2}}(\boldsymbol{\tau}_x \pm \boldsymbol{\tau}_y)\ , & \mu = \pm 1 \\ \boldsymbol{\tau}_z\ , & \mu = 0 \end{cases} \quad (3.9)$$

and $\boldsymbol{\tau}_x$, $\boldsymbol{\tau}_y$ and $\boldsymbol{\tau}_z$ are the Pauli isospin matrices. The expansion of the

central part of the effective interaction is given by

$$V_{pj}^{C} = \frac{2}{\pi} \int_0^\infty q^2 dq \sum_{LSJ} (-1)^{J+S} \; [V_\tau^C(q)\delta_{S,0} + V_{\sigma\tau}^C(q)\delta_{S,1}] \times M_{LSJ}(p) \cdot M_{LSJ}(j) \; , \quad (3.10)$$

and that of the tensor part takes the form

$$V_{pj}^{T} = \frac{2}{\pi} \int_0^\infty q^2 dq \sum_{LL'J} V_\tau^T(q) i^{L+L'+2} \times Z(L', L, J) \; M_{L'1J}(p) \cdot M_{L1J}(j) \; . \quad (3.11)$$

The $Z(L', L, J)$ are geometrical recoupling coefficients, which can be expressed [25] in terms of the total angular momentum transfer J.

For small momentum transfer ($qr < 1$), one can expand the Bessel function $j_L(qr)$ in a Taylor series. One then finds that for $0^+ \rightarrow J^\pi$ transitions, the isovector multipole operators for the lowest multipolarities are given by [26]

$$\sum_j M_{000,\mu}(q\boldsymbol{r}_j) \rightarrow \frac{1}{\sqrt{4\pi}} \sum_j [1 - \frac{(qr_j)^2}{6}] \; \boldsymbol{\tau}_\mu(j) \; , \quad (3.12)$$

$$\sum_j M_{011\mu}(q\boldsymbol{r}_j, \boldsymbol{\sigma}) \rightarrow \frac{1}{\sqrt{4\pi}} \sum_j [1 - \frac{(qr_j)^2}{6}] \; \boldsymbol{\sigma}(j)\boldsymbol{\tau}_\mu(j) \; , \quad (3.13)$$

$$\sum_j M_{101,\mu}(q\boldsymbol{r}_j) \rightarrow \sum_j \frac{i}{3}(qr_j) Y_1(\hat{\boldsymbol{r}}_j)\boldsymbol{\tau}_\mu(j) \; , \quad (3.14)$$

$$\sum_j M_{111,\mu}(q\boldsymbol{r}_j, \boldsymbol{\sigma}) \rightarrow \sum_j \frac{i}{3}(qr_j)[Y_1(\hat{\boldsymbol{r}}_j) \otimes \boldsymbol{\sigma}]^J \boldsymbol{\tau}_\mu(j) \; , \quad (3.15)$$

where the summation is done over the number of nucleons in the target. The operators in eq. 3.12 consist of two parts: the first is proportional to the Fermi operator, while the second corresponds to the isovector monopole operator. The same holds for eq. 3.13, only here the spin operator $\boldsymbol{\sigma}$ is also involved. This leads to the Gamow-Teller (GT) operator for the first part and the spin-isovector monopole operator for the second. The operators in eq. 3.14 and eq. 3.15 are associated with isovector dipole transitions which involve either no spin flip (3.14) or spin flip (3.15). The spin-flip dipole transitions can have spin-parity $J^\pi = 0^-$, 1^- or 2^-, and therefore involve three collective components grouped into the spin-dipole resonance (SDR).

3.3 The spin-dipole resonance (SDR)

The SDR is a 1 $\hbar\omega$ excitation with a change in quantum numbers $\Delta L = \Delta S = \Delta T = 1$, leading to three components representing angular momentum transfers $\Delta J = 0$, 1, 2. Starting from a $J^\pi = 0^+$ ground state, the three components have spin-parity $J^\pi = 0^-$, 1^- or 2^-. The $0^+ \rightarrow 0^-$ transition holds a special place among the spin-dipole transitions because it carries the pion quantum numbers and corresponds to a pure spin-longitudinal transition (see eq. 3.5). The $0^+ \rightarrow 1^-$ spin-dipole transition corresponds to a pure-transverse transition while the $0^+ \rightarrow 2^-$ transition is a mixture of both.

Calculated strength distributions for the SDR based on shell-model calculations for ^{12}B (see figure 3.2) have been performed by Brady *et al.* [8] (using the Millener-Kurath (MK) interaction [27]) and by Olson *et al.* [9] (using the Warburton and Brown (WBT) interaction [28]) and for ^{12}C by Suzuki and Sagawa [29] (using the PSDMKII [30] interaction and the interaction from Kuo [31]). The results of the calculation from Suzuki and Sagawa, assuming isospin symmetry, have just to be shifted by 15.11 MeV since the ^{12}B ground state is the analog of the 15.11 MeV state in ^{12}C. All these calculations predict similar strength distributions for the SDR, with one main 2^- state around 4 MeV excitation energy, a group of 1^- levels around 7-8 MeV excitation energy and 0^- strength fragmented between 4 and 20 MeV, with most strength concentrated around 9 MeV excitation energy.

Experimentally, the three components of the SDR have not yet been resolved, because the interpretation of the results is hampered by the difficulty of identifying contributions from the different J components, since angular distributions are dependent on the orbital angular momentum transfer ΔL, rather than ΔJ. Additional information is needed to separate the different components. One way is to measure the spin-transfer coefficient D_{nn} in the ($\vec{\mathrm{p}}$,$\vec{\mathrm{n}}$) reaction along with ΔL from the angular distribution, which is predicted to provide a unique determination of ΔJ. A measurement of the angular distribution of the particle decay of the SDR would also yield additional information on the different components. Finally, the measurement of tensor analysing powers in a (d,^{2}He) reaction would give the same information as the ($\vec{\mathrm{p}}$,$\vec{\mathrm{n}}$) measurement.

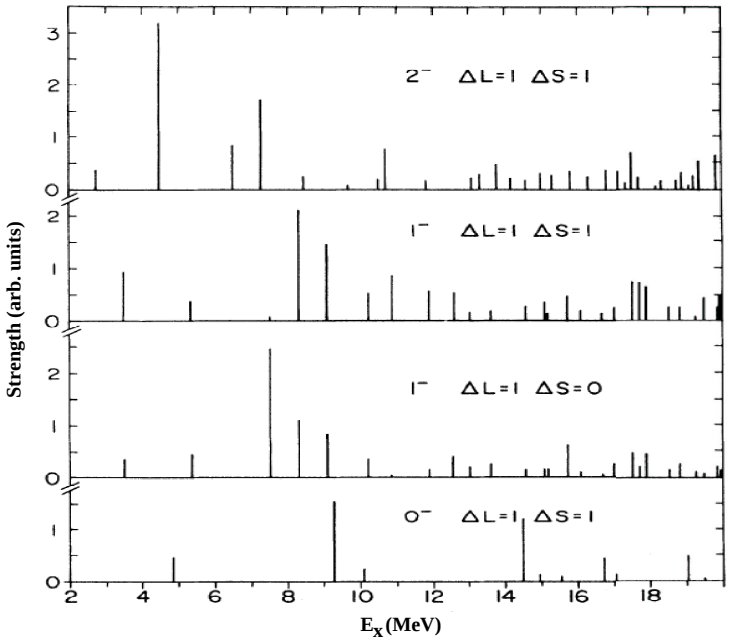

Figure 3.2: Theoretical distribution of dipole and spin-dipole strength as a function of the excitation energy in ^{12}B, taken from ref. [8]. All distributions have the same scale.

3.3.1 Status of the SDR search

The SDR was discovered using the (p,n) reaction on ^{208}Pb at 120 MeV [32]. The properties of the SDR were further investigated by Gaarde *et al.* [33] using the (p,n) reaction on targets of mass $40 \leq A \leq 208$ at 200 MeV. In additon, the SDR has also been studied using the (^{3}He,t) reaction on different Sn isotopes [34, 35, 36]. However, the most serious efforts to study the SDR have been performed on ^{12}C in order to resolve a longstanding controversy concerning the location of the $J^\pi = 0^-, 1^-, 2^-$ states. We will be focusing on these.

Reactions that have been used for studying the SDR on the mass $A = 12$ system are the (p,n) [12, 15, 10, 14, 16], (n,p) [8, 9, 10], (^{3}He,t+p) [11, 6], (d,^{2}He) [6, 5, 7] reactions and a heavy-ion charge-exchange reaction [13].

From all these measurements, it was concluded that the 2^- component of the SDR in ^{12}B was located at 4.5 MeV. The spin and parity assignment of a second bump around 7.5 MeV is still puzzling. Theoretical calculations, (p,n) studies [12, 10] and a measurement of the neutron decay of ^{12}B following the (d,^{2}He) reaction [6] suggest the bump is dominated by 1^- states. However, a dominant contribution of 2^- states is proposed by other groups, based on ($\vec{p}$,$\vec{n}$) measurements [16], tensor analysing power measurements in the (d,^{2}He) reaction [5, 7] and a heavy ion charge-exchange reaction [13]. Ref. [7] also indicates possible evidence for the 0^- state around $E_x = 9.3$ MeV.

3.4 The (d,^{2}He) reaction

The (d,2p) reaction is referred to as (d,^{2}He) when the two protons of the ejectile are in a $^1S_0$ state. It is a charge-exchange reaction exciting the same isospin-raising transitions (β^+) as (n,p)-type reactions, but with additional selectivity in the spin response, which will be addressed later. Although ^{2}He is an unbound state, one assumes it behaves like a real particle and that it decays only after the scattering process, when it is far from the residual nucleus. The distance from the scattering process at which the breakup of ^{2}He into two protons happens can be estimated from the width of the $^1S_0$ state of $\approx$ 1 MeV. Taking a velocity of 0.3 c for the ^{2}He, where c is the speed of light, yields a flight path of $\approx$ 70 fm before decay. At bombarding energies of about 100 MeV/u or higher, the (d,^{2}He) reaction is considered as a one-step reaction.

3.4.1 (n-p)-type reactions

The most used (n,p)-type reactions are the (n,p), (t,^{3}He), (d,^{2}He) and the heavy-ion reactions (^{7}Li,^{7}Be), (^{12}C,^{12}N). The last two reactions suffer from several limitations, among which a rapid increase in momentum transfer with angle (difficulty in discriminating different ΔL transfers) and a need for high-energy beams to ensure a one-step reaction (limitation in energy resolution).

The other (n,p)-type reactions also come with their share of experimental problems. The (n,p) reaction at intermediate energies suffers from the limited energy resolution ($\approx$ 1 MeV) and intensity ($\approx 10^6$ n/s) of the secondary beam, while the production of a primary tritium beam for the (t,^{3}He) reaction is confronted with safety regulations if one wants to obtain high intensities. The (d,^{2}He) reaction imposes severe conditions on the detection

system, especially close to (and at) 0°, where the two correlated protons are emitted in close geometry among a huge quantity of uncorrelated protons stemming from the Coulomb break up of the incoming deuterons on the target.

3.4.2 Measuring the (d,^{2}He) reaction

Since the ^{2}He is in a $^1S_0$ state, it will decay isotropically in its centre-of-mass frame. When one performs the Lorentz transformation to the laboratory system, the relative angle between the two protons decreases, depending on the kinematics of the reaction. The higher the incoming beam energy, the smaller the relative angle. This means that above a certain incident energy, a magnetic spectrometer is perfectly suited to detect the ^{2}He particles with a high efficiency, since the two protons from the ^{2}He are emitted in a narrow cone.

An important quantity measured with the (d,^{2}He) reaction is the internal energy ϵ of the diproton system. The energy ϵ is given by using by the four-momenta $P_i^\mu = (E_i, \boldsymbol{p}_i)$ of the two protons

$$\epsilon = \sqrt{2\left(m_p^2 + E_1 E_2 - |\boldsymbol{p}_1||\boldsymbol{p}_2| cos(\theta_{pp})\right)} - 2m_p \ , \tag{3.16}$$

where m_p is the proton mass and θ_{pp} the relative angle between the two protons. The internal energy is a measure of the contribution of higher order partial waves in the p-p system. It was shown [37] that for an internal energy ϵ below 1 MeV, the ^{2}He system is in a well defined $^1S_0$ state and that contributions from higher partial waves are negligibly small.

3.4.3 Selectivity of the reaction

The (d,^{2}He) reaction forces a spin-flip and isospin-flip transition ($\Delta S = \Delta T = 1$) because the deuteron and ^{2}He have spin-isospin values of (1,0) and (0,1), respectively. The D-state admixture ($\approx 4\%$) of the deuteron wave function is neglected at this point.

In N>Z nuclei, the (d,^{2}He) reaction excites exclusively states with isospin $T_0 + 1$. The selectivity of the (d,^{2}He) reaction makes it particularly useful for the determination of Gamow-Teller (GT) strength, since it fulfills all the requirements of the selection rules for small momentum transfer (see eq. 3.13).

However, if one uses a purely tensor-polarised deuteron beam, the (d,^{2}He) reaction becomes a unique tool for the study of spin phenomena. The tensor

analysing powers correspond to information that can be obtained in a much more difficult spin-transfer experiment in the $(\vec{n}, \vec{p})$ reaction [3].

3.4.4 DWBA treatment of the reaction

Generally, data obtained from scattering experiments are analysed using the distorted-wave Born approximation (DWBA). The differential cross section for a reaction $A(a,b)B$ corresponding to a transition from an initial state i to a final state f is given by [38]

$$\frac{d\sigma_{fi}}{d\Omega} = \frac{\mu_i \mu_f}{(2\pi\hbar^2)^2} \frac{k_f}{k_i} |T_{fi}|^2 , \tag{3.17}$$

where μ_i and μ_f are the reduced masses in the initial and final states, k_i and k_f are the wave numbers of the incoming and outgoing waves, respectively. T_{fi} is the transition amplitude. A quantity related to the transition amplitude is the scattering amplitude M defined by

$$M_{fi} = - \frac{\sqrt{\mu_i \mu_f}}{2\pi\hbar^2} \sqrt{\frac{k_f}{k_i}} T_{fi}. \tag{3.18}$$

In case ^{2}He were in a bound state, the transition amplitude looks like [5]

$$T^{DWBA} = < \chi^{(-)}_{^2\mathrm{He}} \; \psi_{^2\mathrm{He}} \; \Psi_{A^*} | V | \chi^{(+)}_d \; \varphi_d \; \Psi_A >, \tag{3.19}$$

where the projectile and ejectile wave functions of the incident- and exit-channels are denoted by φ_d and $\psi_{^2\mathrm{He}}$, the target wave functions by Ψ_A and Ψ_{A^*} and the distorted waves by $\chi^{(+)}_d$ and $\chi^{(-)}_{^2\mathrm{He}}$, respectively.

However, in the (d,^{2}He) reaction, one has to deal with a three-body problem in the outgoing channel, since ^{2}He is an unbound state. If one uses a standard DWBA technique, like the one presented in eq. 3.19, the imaginary part of the optical potential for the outgoing wave has to be arbitrarily searched for to fit the data, leading to ambiguities when interpreting the results [39].

The adiabatic approximation

A method to treat the three-body dynamics of the (d,^{2}He) reaction was formulated by Okamura in the adiabatic approximation [40], which had been

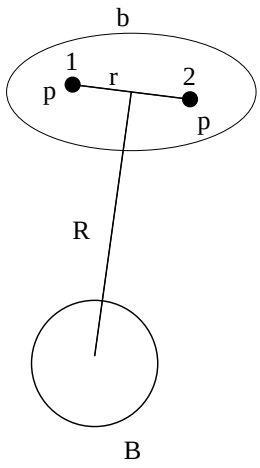

Figure 3.3: Coordinates of the three-body system p-p-B, where B is the residual nucleus and b the p-p system.

successfully applied to the (^{3}He,^{2}He) reaction [41]. The Schrödinger equation for the three-body system is given by

$$\left(-\frac{\hbar^2}{2\mu_{bB}}\Delta_R + V_{1B}(\mathbf{r},\mathbf{R}) + V_{2B}(\mathbf{r},\mathbf{R}) + H_{12} - E\right)\Psi(\mathbf{K}_f,\mathbf{k};\mathbf{r},\mathbf{R}) = 0\ . \tag{3.20}$$

Here, $\mathbf{R}$ represents the relative coordinate between the centre of mass of the ejectile system and the residual nucleus, $\mathbf{r}$ the relative coordinate between the two protons, as shown in fig. 3.3, $\mathbf{K}_f$ and $\mathbf{k}$ are the asymptotic wave numbers in the exit channel.

The basic idea behind the adiabatic approximation resides in neglecting the excitation of the diproton system when constructing the final three-body wave function. This is done by replacing the sub-Hamiltonian H_{12} by its eigenvalue, the relative energy ϵ. Furthermore, the sum of the two potentials $V_{iB}(\mathbf{r},\mathbf{R})$ is replaced by a sum of two optical potentials $U_{iB}(\mathbf{r},\mathbf{R})$ evaluated at $\frac{1}{2}(E-\epsilon)$, which yields

$$\left(\Delta_R - \frac{2\mu_{bB}}{\hbar^2}(U_{1B}(\mathbf{r},\mathbf{R}) + U_{2B}(\mathbf{r},\mathbf{R})) + K_f^2\right)\Psi_{ad}(\mathbf{K}_f,\mathbf{k};\mathbf{r},\mathbf{R}) = 0\ , \tag{3.21}$$

where

$$K_f^2 = \frac{2\mu_{bB}}{\hbar^2}(E-\epsilon)\ , \tag{3.22}$$

and $\Psi_{ad}(\mathbf{K}_f,\mathbf{k};\mathbf{r},\mathbf{R})$ is the adiabatic three-body wave function.

The T-matrix is now

$$T^{ad}(\mathbf{k}, \mathbf{K}_i, \mathbf{K}_f) = < \Psi^-_{ad} \, |F| \, \chi^{(+)}_d \, \varphi_d > , \tag{3.23}$$

in which F is the target form factor

$$F(\boldsymbol{R}, \boldsymbol{r}) = < \Phi_B | \sum_{p,j} V_{pj} | \Phi_A > \tag{3.24}$$

describing the nuclear response using the effective interaction between nucleons in the target and projectile. Φ_A and Φ_B denote the target ground state and the final state of the rest nucleus, respectively. The advantage of this method is that there is no need to define a ^{2}He optical potential.

A detailed discussion of the application of the adiabatic approximation to the (d,^{2}He) reaction can be found in ref. [39], while ref. [42] gives another theoretical method based on the eikonal approximation, including the three-body treatment of both entrance and exit channels.

3.4.5 Symmetry of the transition amplitude

Transition amplitudes have various symmetry properties resulting from the invariance of the Hamiltonian to rotations (conservation of angular momentum) and inversion of the coordinate axes (conservation of parity). These properties allow one to extract information on experimental observables.

In the helicity frame (see figure 2.1), the scattering plane is defined by the two momenta $\boldsymbol{k}_{in}$ and $\boldsymbol{k}_{out}$. The y-axis is then the perpendicular to the scattering plane. Reflection with respect to the scattering plane (x-z plane) is accomplished by the combined action of the parity and rotation operators and yields the following symmetry relation [38]

$$|\boldsymbol{k}; IM > = \pi \, (-1)^{I-M} \, |\boldsymbol{k}; I - M > , \tag{3.25}$$

where π is the intrinsic parity of the particle, I its spin and M its z-projection.

Applying eq. 3.25 to the transition matrix T for an $A(a,b)B$-type reaction yields

$$\begin{aligned} &< I_B M_B I_b M_b | T | I_A M_A I_a M_a > = \\ &\qquad (-1)^{\eta_{fi}} \, \pi_{fi} \; < I_B - M_B I_b - M_b | T | I_A - M_A I_a - M_a > , \end{aligned} \tag{3.26}$$

where π_{fi} is the overall change in intrinsic parity

$$\pi_{fi} \;=\; \pi_B \pi_b \pi_A \pi_a \; , \tag{3.27}$$

and η_{fi} is the phase

$$\eta_{fi} = I_B - M_B + I_b - M_b + I_A - M_A + I_a - M_a \ . \tag{3.28}$$

3.4.6 Polarisation observables

For the (d,^{2}He) reaction on an even-even target, for which $I_A^{\pi_A} = 0^+$, $I_a^{\pi_a} = 1^+$ and $I_b^{\pi_b} = 0^+$, the T matrix has only $< M_B|T|M_a >$ components, and model-independent relations concerning the tensor analysing powers given by

$$A_{ij} = \frac{Tr(TP_{ij}T^\dagger)}{Tr(TT^\dagger)} \tag{3.29}$$

can be derived.

For a 0^- state, $I_B^{\pi_B} = 0^-$ and eq. 3.26 leads to

$$< M_B = 0|T|M_a = 1 >= - \ < M_B = 0|T|M_a = -1 > . \tag{3.30}$$

Inserting this into the expression for the analysing power eq. 3.29 gives

$$A_{ij} = \frac{\sum_{M_B M_a M_a'} < M_B|T|M_a >< M_a|P_{ij}|M_a' >< M_a'|T|M_B >^*}{\sum_{M_B M_a} | < M_B|T|M_a > |^2} \tag{3.31}$$

and using P_{yy} as operator yields

$$A_{yy} = 1 \quad \text{for a } 0^- \text{ state,} \tag{3.32}$$

irrespective of the scattering angle and model independently.

Furthermore, still for a 0^- state, using the same method as above, it can be shown that[1]

$$A_{zz} + A_{xx} - A_{yy} = -2 \quad \text{for a } 0^- \text{ state,} \tag{3.33}$$

again, irrespective of the scattering angle and model independently.

At 0° (or 180°), the T-matrix is rotationally invariant around the beam axis, meaning $[J_z, T] = 0$ and one can deduce

$$< M_B|[J_z, T]|M_a >= (M_B - M_a) \ < M_B|T|M_a >= 0. \tag{3.34}$$

This yields

$$A_{zz} = -2 \quad \text{for a } 0^- \text{ state at } 0^\circ. \tag{3.35}$$

[1] This can also be derived by inserting the result from eq. 3.32 in eq. A.15

Additionally, one sees that A_{xx} and A_{yy} are equal at 0°. For natural parity states, $\pi_B = (-1)^{I_B}$ and eq. 3.26 becomes

$$< M_B|T|M_a >= (-1)(-1)^{M_B+M_a} \ < -M_B|T| - M_a > . \tag{3.36}$$

This last result tells us that the only non-zero components of the T-matrix are for $M_B = M_a = \pm 1$, resulting in

$$A_{zz}(0^\circ) = 1 \text{ and } A_{xx}(0^\circ) = A_{yy}(0^\circ) = -\frac{1}{2} \tag{3.37}$$

for natural-parity states at exactly 0°.